

Depth-Dependent Magnetization Profiles of Hybrid Exchange Springs

T. N. Anh Nguyen,^{1,2,*} R. Knut,³ V. Fallahi,⁴ S. Chung,^{1,5} Q. Tuan Le,¹ S. M. Mohseni,^{1,6} O. Karis,³ S. Peredkov,⁷ R. K. Dumas,⁵ Casey W. Miller,⁸ and J. Åkerman^{1,5,9}

¹Materials and Nano Physics, School of ICT, Royal Institute of Technology, Electrum 229, 164 40 Kista, Sweden

²Spintronics Research Group, Laboratory for Nanotechnology,

Vietnam National University-Ho Chi Minh City, Ho Chi Minh City, Vietnam

³Department of Physics and Astronomy, Uppsala University, Box 516, 75120, Sweden

⁴Faculty of Physics, Amirkabir University of Technology, Hafez Avenue, 1591634311 Tehran, Iran

⁵Department of Physics, University of Gothenburg, 412 96 Gothenburg, Sweden

⁶Department of Physics, Shahid Beheshti University, Tehran, Iran

⁷Max-lab, Lund University, Box 118, 22100 Lund, Sweden

⁸School of Chemistry and Materials Science, Rochester Institute of Technology,

85 Lomb Memorial Drive, Rochester, New York 14623, USA

⁹NanOsc AB, Electrum 205, 164 40 Kista, Sweden

(Received 28 August 2014; published 24 October 2014)

We report on the magnetization depth profile of a hybrid exchange-spring system in which a Co/Pd multilayer with perpendicular anisotropy is coupled to a CoFeB thin film with in-plane anisotropy. The competition between these two orthogonal anisotropies promotes a strong depth dependence of the magnetization orientation. The angle of the magnetization vector is sensitive both to the strength of the individual anisotropies and to the local exchange constant and is thus tunable by changing the thickness of the CoFeB layer and by substituting Ni for Pd in one layer of the Co/Pd stack. The resulting magnetic depth profiles are directly probed by element-specific x-ray magnetic circular dichroism of the Fe and Ni layers located at different average depths. The experimental results are corroborated by micromagnetic simulations.

DOI: 10.1103/PhysRevApplied.2.044014

I. INTRODUCTION

The phenomenon of spin-transfer torque [1–3] has brought about applications such as spin torque oscillators [4–7] and spin-transfer torque-based magnetoresistive random access memory (MRAM) [8,9]. These devices were initially based on magnetic materials with in-plane magnetic anisotropy, which lead to unnecessarily high spin-transfer torque-MRAM switching currents, poor memory retention, poor scalability [10], and high-field requirements for spin torque oscillators [11]. Spin-transfer torque devices based on perpendicular magnetic anisotropy materials have proven more advantageous due to low switching currents, high switching speeds, good thermal stability, future scalability [8,12–14], and low- to zero-field operation of spin torque oscillators [15–19].

A natural extension of perpendicular anisotropy is materials in which the magnetization is *tilted* with respect to the surface normal. Such materials allow for additional control of the magnetization dynamics in magnetic nanostructures [20–22] and suggest the possibility of improved spin-transfer torque-MRAM switching behavior

and thermal stability [23–26] and spin torque oscillator devices [20–22,26–30]. Materials with tilted magnetic anisotropies have been realized by using collimated oblique sputtering [31], depositing multilayers on nanospheres [23], and exploiting crystallographic texture [32–34]. A more versatile approach was recently reported using hybrid exchange springs, structures that combine materials with out-of-plane and in-plane magnetic anisotropies to enable wide and tunable ranges of magnetization tilt angles [35–37]. By using different layer thicknesses and coupling strengths, the average tilt angle, and even the damping, can be varied. However, details of the highly nonlinear magnetization through these structures are only indirectly inferred [35–37]. Magnetic depth profiles of systems whose tunability originates from indirect coupling between the perpendicular and in-plane layers [38] are studied by soft-x-ray resonant magnetic reflectivity [39], x-ray magnetic circular dichroism (XMCD) [40,41], and polarized neutron reflectometry [42,43].

In this work, we present a depth-resolved study of the spin orientation in strongly coupled hybrid exchange springs using XMCD. The depth resolution is obtained by using the elemental specificity of XMCD to separately probe both a Ni layer that was inserted at various depths in the perpendicular stack and Fe that is found only in the

*To whom correspondence should be addressed.
anhntn@kth.se

in-plane anisotropy layer. This technique provides the necessary experimental information to verify the depth-dependent magnetization obtained from micromagnetic simulations.

II. EXPERIMENT

The studied exchange springs have a top $\text{Co}_{40}\text{Fe}_{40}\text{B}_{20}$ (CoFeB) layer with in-plane anisotropy, which is grown onto a Co/Pd multilayer stack that has perpendicular magnetic anisotropy. CoFeB is chosen for being magnetically soft and the material of choice for exchange springs in magnetic tunnel junctions. A Ta(10 nm)/Pd(3 nm) seed layer is used to improve the perpendicular anisotropy of the Co/Pd [44,45]. To tune the properties of the exchange spring, we prepare two sample types: series A has a fixed CoFeB thickness (1.75 nm) with a Co/Ni bilayer located at different positions (n) within the perpendicular stack: $[\text{Co}/\text{Pd}]_{4-n}/\text{Co}/\text{Ni}/[\text{Co}/\text{Pd}]_n/\text{CoFeB}(1.75 \text{ nm})$; in series B, n is fixed at 2, while the CoFeB thickness (t_{CoFeB}) is deposited as a wedge ($0.5 \text{ nm} \leq t_{\text{CoFeB}} \leq 1.75 \text{ nm}$) using oblique deposition: $[\text{Co}/\text{Pd}]_2/\text{Co}/\text{Ni}/[\text{Co}/\text{Pd}]_2/\text{CoFeB}(t_{\text{CoFeB}})$. A set of control samples of the form $[\text{Co}/\text{Pd}]_5/\text{CoFeB}(0.5 \text{ nm})$ and $[\text{Co}/\text{Pd}]_{4-n}/\text{Co}/\text{Ni}/[\text{Co}/\text{Pd}]_n/\text{CoFeB}(0.5 \text{ nm})$ ($n = 0, 1, \text{ and } 2$) are also measured. All Ni, Co, and Pd layers are 1, 0.5, and 1.8 nm thick, respectively. All samples are sputter deposited at room temperature on Si/SiO₂ substrates and are protected from oxidization by a 2-nm Ta capping layer. Magnetization measurements are made at room temperature by using an alternating gradient magnetometer with the magnetic field in the plane (M_x -vs- H loops) and separately with the field along the surface normal (M_z -vs- H loops).

Substituting one Ni layer for one Pd layer changes the magnetic properties of the perpendicular stack. Figure 1 shows that this change reduces the coercive field (H_C), as expected for exchange-coupled composite structures [46,47]. When the Ni layer is positioned deeper within

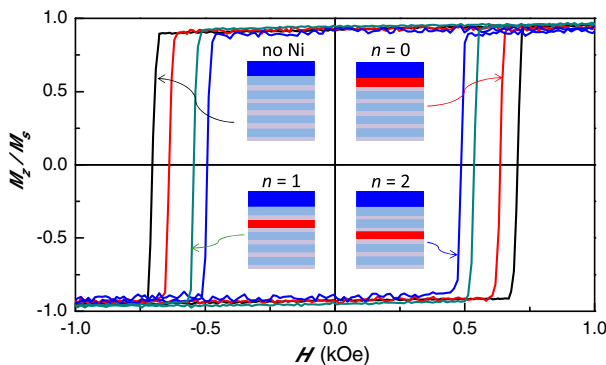


FIG. 1. M_z -vs- H loops for $[\text{Co}/\text{Pd}]_{4-n}/\text{Co}/\text{Ni}/[\text{Co}/\text{Pd}]_n/\text{CoFeB}(0.5 \text{ nm})$ ($n = 0, 1, \text{ and } 2$) and Ni-free $[\text{Co}/\text{Pd}]_5/\text{CoFeB}(0.5 \text{ nm})$ hybrid exchange springs indicate robust perpendicular anisotropy.

the stack, the Co/Pd is effectively separated into two parts, resulting in a monotonic decrease of H_C from the control sample's value of approximately 680 Oe down to approximately 480 Oe. Even with this reduction in H_C , a strong perpendicular anisotropy with a well-defined square loop and narrow switching field distribution is always observed. The M_x -vs- H loops (not shown) reveal relatively large saturation fields of about 1 T for all samples, demonstrating the strong perpendicular anisotropy.

Increasing the thickness of the CoFeB layer puts the in-plane anisotropy into competition with the perpendicular anisotropy of the underlying stack. The M_z -vs- H and M_x -vs- H hysteresis loops for samples with $t_{\text{CoFeB}} = 0.5, 0.85, 1, 1.25, \text{ and } 1.75 \text{ nm}$ are shown in Figs. 2(a) and 2(b), respectively. The data reveal a dramatic effect on the magnetization reversal as t_{CoFeB} is increased. A significant out-of-plane remanence is retained for $t_{\text{CoFeB}} = 0.5 \text{ nm}$, consistent with rigid coupling of the CoFeB layer to the perpendicular stack. However, the in-plane anisotropy of the CoFeB layer begins to dominate as t_{CoFeB} is increased, reducing the remanence and increasing the saturation field in the M_z -vs- H loops.

XMCD measurements allow us to probe with elemental specificity the depth dependence of the magnetization within the exchange spring. Thus, by focusing on the Fe and Ni signals, we can selectively probe the different regions of the heterostructure; in principle, this method is also possible with Co, but becomes complicated because it is present throughout the structure, and is thus not treated here. The XMCD spectra (taken at MAX-Lab beam lines I1011 and D1011) are taken at the L_3 edges of Ni and Fe at varying angles between the incident x ray and the remanent sample magnetization. All samples are fully magnetized out of plane and then measured at remanence by using the total electron yield. The difference in absorption between left- and right-circularly-polarized light in magnetic materials leads to an asymmetry that is proportional to the

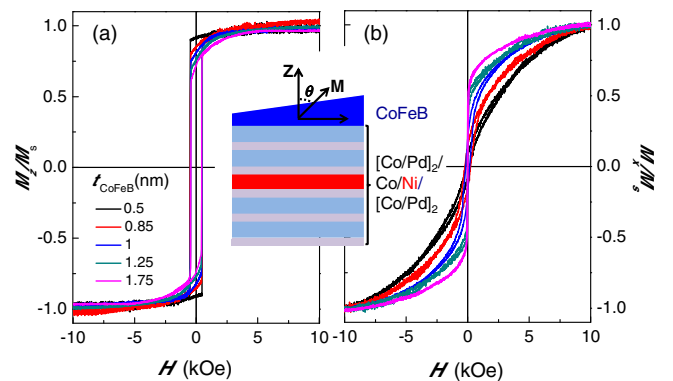


FIG. 2. (a) M_z -vs- H and (b) M_x -vs- H loops from hybrid exchange springs of the form $[\text{Co}/\text{Pd}]_2/\text{Co}/\text{Ni}/[\text{Co}/\text{Pd}]_2/\text{CoFeB}(t_{\text{CoFeB}})$ show that in-plane anisotropy competes with perpendicular anisotropy with increasing t_{CoFeB} , which enables a tunable tilt angle for the magnetization vector.

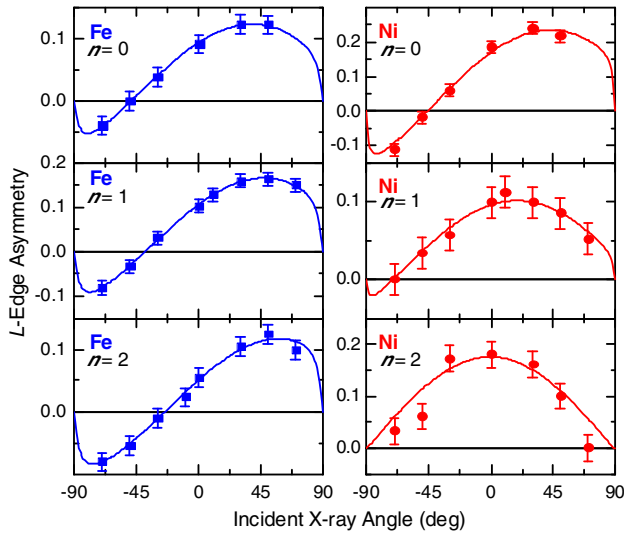


FIG. 3. Asymmetry of Fe L_3 (left column) and Ni L_3 absorption edges (right column) as a function of angle between the incident x rays and the surface normal. The samples belong to series A, with a 1.75-nm CoFeB top layer and different depths of the Co/Ni bilayer ($n = 0, 1, 2$). The CoFeB magnetization becomes more in plane with Co/Ni depth, while that of Ni becomes more out of plane.

magnetization. The asymmetry depends on the angle of incidence, which allows the average magnetization direction of each element to be determined. The asymmetry is proportional to the projection of the spin magnetic moment on the direction of the incident x rays. The direction of the average magnetic moment is thus given by the peak value; equivalently and easier in practice, the zero crossing of the asymmetry indicates the angle orthogonal to the average magnetization. Figure 3 shows the Fe L_3 and Ni L_3 asymmetries vs the angle between the incident x rays and the surface normal. The data are fitted by the function $\cos(x - \theta)S(x)$, where x is the angle between the surface normal and the incident light and θ is the angle of the magnetization relative to the normal; $S(x)$ corrects for saturation effects [48]. Since the zero crossing for the Fe asymmetry tends toward 0° with increasing n , the CoFeB anisotropy is increasingly in plane as the Ni is placed deeper into the stack. The zero crossing for Ni moves away from 0° with n , thus indicating an increased perpendicular character.

It is important to note that the XMCD asymmetry at the L_3 edge is sensitive to the magnetic dipole term and orbital magnetic moment [49,50]. Combining the spin and orbital moment sum rules, it is found that the asymmetry of the L_3 absorption edge in $3d$ transition metals is proportional to approximately $m_S + m_D + 3m_{\text{orb}}$, where m_S is the isotropic spin magnetic moment, m_D is the magnetic dipole term, and m_{orb} is the orbital magnetic moment [51–53]. The dipole term can be expanded as $m_D = m_D^\perp \cos(\varphi) + m_D^\parallel \sin(\varphi)$, where m_D^\perp and m_D^\parallel are the out-of-plane and in-plane components of m_D , respectively,

and φ is the angle of the spin magnetic moment relative to the out-of-plane direction [54]. An identical relation can be made for the orbital moment by using m_{orb}^\perp and m_{orb}^\parallel . To a good approximation, $m_D^\perp + 2m_D^\parallel = 0$ for $3d$ metals without in-plane anisotropy [55,56], and hence knowledge of only one component is sufficient. Theoretical calculations of m_D^\perp for free interfaces in Fe and Ni are given by Wu and Freeman [53], and the calculated deviation ($\leq 3^\circ$) in the measured m_S angle due to m_D^\perp for Fe and Ni for all samples has been accounted for. The m_{orb} for Fe and Ni interfaces [57] are sufficiently small relative to m_D that they can be neglected. The remanent in-plane magnetization direction is determined by additional measurements for different azimuthal angles of the sample. Deviations between the remanent magnetization direction and the plane studied in the angular scans are compensated for in the derivation of out-of-plane angles.

The XMCD results reveal a wide variation between the magnetization tilt angles θ_M for Fe and Ni within the exchange springs. Figure 4 illustrates the CoFeB thickness and Ni depth dependences of the tilted angles in Fe (present only in the CoFeB) and Ni (present only in one depth location in the exchange spring). For very thin CoFeB samples ($t_{\text{CoFeB}} < 1$ nm), all layers maintain perpendicular anisotropy due to the rigid coupling between the CoFeB layer and the perpendicular stack. However, the stronger in-plane anisotropy of thicker CoFeB ($t_{\text{CoFeB}} > 1$ nm) causes the magnetic moments of the Fe to tilt away from the surface normal. For example, the magnetic moment of Fe within the thickest CoFeB layer is tilted 73° due to the dominant in-plane anisotropy. Analysis as a function of Ni depth shows that the CoFeB and Ni are directly

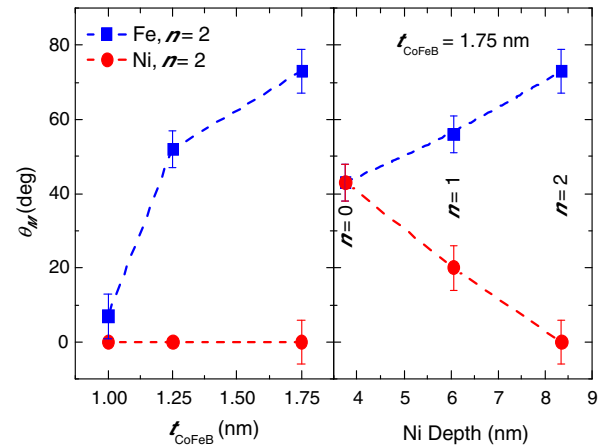


FIG. 4. Measured magnetization tilt angles θ_M for Fe and Ni as functions of t_{CoFeB} (a) and Ni depth (b) for different positions of the Co/Ni bilayer within the perpendicular stack. Lines are fits, as described in the text. The different angles for Fe and Ni within one sample indicate that the magnetization tilt angle changes within the structure; this tilt-angle gradient is thus tunable by both CoFeB thickness and position of the Co/Ni layer.

coupled for $n = 0$ (Ni depth = 3.75 nm) and exhibit the same angle of 43° . This coupling is modified for $n = 1$ and 2. A deep Ni layer ($n = 2$) aligns out of plane, with an intermediate tilt observed for $n = 1$. The discrepancy between the tilt angles for Fe and Ni for $n = 1$ and 2 indicates that the internal magnetization acquires an angle gradient within the structure; i.e., the local magnetization has a nontrivial depth-dependent orientation relative to the surface normal. The $n = 2$ sample data in Fig. 4(b) show that the magnitude of this angle gradient is set by the CoFeB thickness; a large dynamic range is possible.

III. MICROMAGNETICS

Micromagnetic simulations that quantitatively determine the magnetization tilting within the various magnetic layers are fully consistent with our XMCD results. The calculations are based on a 1D micromagnetic model [33,37] in which the depth dependence of the magnetic configuration is calculated by minimizing Gibb's free energy:

$$G = - \sum_{i=1}^{N_1+N_2+N_3+N_4-1} \frac{A_{i,i+1}^{\text{ex}}}{d_{i,i+1}} \cos(\theta_{i+1} - \theta_i) + \sum_{i=1}^{N_1+N_2+N_3+N_4} \left(K_i - \frac{1}{2} \mu_0 M_i^2 \right) \sin^2(\theta_i) - \sum_{i=1}^{N_1+N_2+N_3+N_4} \mu_0 H M_i \cos(\theta_i),$$

taking into account the exchange, anisotropy, and Zeeman energies. N_1 , N_2 , N_3 , and N_4 are the number of monolayers which refer to $[\text{Co}/\text{Pd}]_{4-n}$, $[\text{Co}/\text{Ni}]$, $[\text{Co}/\text{Pd}]_n$, and CoFeB layers, respectively. The layer thickness d_i , exchange stiffness between two nearest-neighbor monolayers $A_{(i,i+1)}$, anisotropy K_i , and saturation magnetization M_i are used as material-specific input parameters; θ_i is the angle between the z axis and the magnetization. The equilibrium state is determined by optimizing the coupled nonlinear equations with the Weierstrass-Erdmann boundary conditions [58]. The $[\text{Co}/\text{Pd}]$ multilayer is treated as a continuous slab with $A_i^{\text{ex}} = 2$ pJ/m, $K_i = 0.15$ MJ/m³, and $M_i = 0.355$ A/m for $i \leq N_1$ and $N_2 \leq i \leq N_3$. M_i is directly extracted from the magnetometry of a $[\text{Co}/\text{Pd}]_5$ stack. The exchange stiffness for the Co/Ni layer is estimated to be 12 pJ/m, consistent with $A \sim 10$ pJ/m for Co-based films. Following reported values [18,37] and the layer-thickness dependence of M_S and K_u commonly seen in perpendicular anisotropy materials [59,60], we use a saturation magnetization and an anisotropy constant of 0.75 MA/m and 0.6 MJ/m³, respectively. Material parameters used for the CoFeB are $K = 0$ pJ/m, $M_S = 0.625 + 0.0875 t_{\text{CoFeB}}$ (nm) MA/m, and $A_i^{\text{ex}} = 19$ pJ/m. Accurately modeling the thickness dependence of M_S for the CoFeB is critical because of the strong dependence

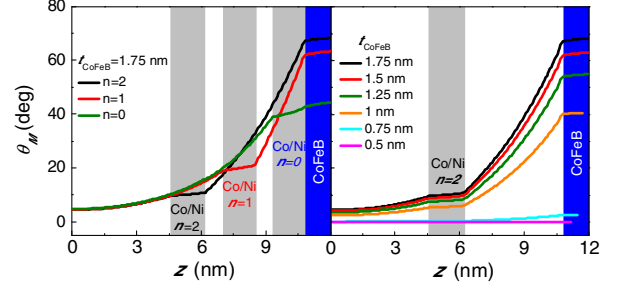


FIG. 5. Micromagnetic results for the tilt angle of the local magnetization, $\theta_M(z)$, within the exchange springs of (a) series A (fixed CoFeB thickness) and (b) series B (varied CoFeB thickness). The gray vertical regions indicate the position of the Co/Ni bilayer; the blue region is the CoFeB. The angle gradient observed with the XMCD experiments is corroborated by these simulations.

of in-plane anisotropy on CoFeB thickness. We determine this parameter by using ferromagnetic resonance measurements of individual CoFeB films; our results are in agreement with prior work [61].

Figure 5 summarizes the calculated tilt angle of the magnetization through the entire exchange spring for series A and B. The tilt angle is engineered by placing the Ni at different locations within the perpendicular stack [Fig. 5(a)]. The tilt angle at the position of the Ni layer closer to the CoFeB becomes larger: angles of 40° , 19° , and 8° are calculated for $n = 0, 1$, and 2 , respectively. Consistent with the experimentally observed reduction in perpendicular anisotropy as the Ni insertion layer moves deeper into the $[\text{Co}/\text{Pd}]$, the tilt angle of the magnetization of the CoFeB layer progressively increases with respect to the surface normal: angles of 44° , 63° , and 69° are calculated for $n = 0, 1$, and 2 , respectively. Moreover, in series B, the simulation results in Fig. 5(b) show that the magnetization tilt angle can be tuned freely as a function of t_{CoFeB} , as previously noted [35,37]. Within the transition region, $0.5 \text{ nm} \leq t_{\text{CoFeB}} \leq 1.75 \text{ nm}$, a clear tilting of θ_M from 0° to 69° is found, consistent with the remanence values. The magnetization configuration is primarily out of plane (0°) for $t_{\text{CoFeB}} < 1$ nm and gradually becomes more in plane with increasing t_{CoFeB} .

IV. CONCLUSIONS

In summary, the magnetization in $[\text{Co}/\text{Pd}]_{4-n}/\text{Co}/\text{Ni}/[\text{Co}/\text{Pd}]_n/\text{CoFeB}$ exhibits strong tilt-angle gradients, extending throughout the exchange spring. The achievable tilt angles cover a wide range, with the top CoFeB angle tunable from 0° to 73° by varying its thickness. The magnetization profile can be further tuned by the position of a Ni layer in the perpendicular stack, with a deeper Ni position increasing the CoFeB tilt angle. The experimental depth profiles of the magnetization in hybrid exchange springs are obtained by using element-specific

XMCD. Micromagnetic calculations corroborate our experimental results and provide a detailed description of the magnetization profile. The results presented here utilize blanket exchange-spring films to demonstrate the ability to accurately tune, and measure, the magnetization tilt angle by taking advantage of competing anisotropies. Utilization of such tilted anisotropy materials in devices such as spin-transfer torque-MRAM and spin torque oscillators is expected to have a significant impact on future magnetic storage and logic technologies.

ACKNOWLEDGMENTS

This work is supported by the European Commission Seventh Framework Programme Contract No. ICT-257159 “MACALO,” the Swedish Foundation for Strategic Research, the Swedish Research Council (VR), and the Knut and Alice Wallenberg Foundation; T. N. A. N. acknowledges support from the National Foundation for Science and Technology Development (NAFOSTED) of Vietnam via Project No. 103.02-2010.27 and the Korea Institute of Science and Technology-International R&D Academy (KIST-IRDA) via Alumni Project No. 2Z03750. C. W. M. acknowledges support from the U.S. NSF.

-
- [1] J. C. Slonczewski, Current-driven excitation of magnetic multilayers, *J. Magn. Magn. Mater.* **159**, L1 (1996).
- [2] L. Berger, Emission of spin waves by a magnetic multilayer traversed by a current, *Phys. Rev. B* **54**, 9353 (1996).
- [3] D. C. Ralph and M. D. Stiles, Spin transfer torques, *J. Magn. Magn. Mater.* **320**, 1190 (2008).
- [4] I. N. Krivorotov, N. C. Emley, J. C. Sankey, S. I. Kiselev, D. C. Ralph, and R. A. Buhrman, Time-domain measurements of nanomagnet dynamics driven by spin-transfer torques, *Science* **307**, 228 (2005).
- [5] S. Kaka, M. R. Pufall, W. H. Rippard, T. J. Silva, S. E. Russek, and J. A. Katine, Mutual phase-locking of microwave spin torque nano-oscillators, *Nature (London)* **437**, 389 (2005).
- [6] W. Rippard, M. Pufall, S. Kaka, S. Russek, and T. J. Silva, Direct-current induced dynamics in Co₉₀Fe₁₀/Ni₈₀Fe₂₀ point contacts, *Phys. Rev. Lett.* **92**, 027201 (2004).
- [7] S. Bonetti, V. Tiberkevich, G. Consolo, G. Finocchio, P. Muduli, F. Mancoff, A. Slavin, and J. Åkerman, Experimental evidence of self-localized and propagating spin wave modes in obliquely magnetized current-driven nano-contacts, *Phys. Rev. Lett.* **105**, 217204 (2010).
- [8] S. Mangin, D. Ravelosona, J. A. Katine, M. J. Carey, B. D. Terris, and E. E. Fullerton, Current-induced magnetization reversal in nanopillars with perpendicular anisotropy, *Nat. Mater.* **5**, 210 (2006).
- [9] C. Chappert, A. Fert, and F. N. Van Dau, The emergence of spin electronics in data storage, *Nat. Mater.* **6**, 813 (2007).
- [10] J. Zhu, Magnetoresistive random access memory: The path to competitiveness and scalability, *Proc. IEEE* **96**, 1786 (2008).
- [11] T. J. Silva and W. H. Rippard, Developments in nano-oscillators based upon spin-transfer point-contact devices, *J. Magn. Magn. Mater.* **320**, 1260 (2008).
- [12] S. Ikeda, K. Miura, H. Yamamoto, K. Mizunuma, H. D. Gan, M. Endo, S. Kanai, J. Hayakawa, F. Matsukura, and H. Ohno, A perpendicular-anisotropy CoFeB-MgO magnetic tunnel junction, *Nat. Mater.* **9**, 721 (2010).
- [13] H. Meng and J.-P. Wang, Spin transfer in nanomagnetic devices with perpendicular anisotropy, *Appl. Phys. Lett.* **88**, 172506 (2006).
- [14] S. Mangin, Y. Henry, D. Ravelosona, J. A. Katine, and E. E. Fullerton, Reducing the critical current for spin-transfer switching of perpendicularly magnetized nanomagnets, *Appl. Phys. Lett.* **94**, 012502 (2009).
- [15] X. Zhu and J.-G. Zhu, Bias-field-free microwave oscillator driven by perpendicularly polarized spin current, *IEEE Trans. Magn.* **42**, 2670 (2006).
- [16] D. Houssameddine, U. Ebels, B. Delaët, B. Rodmacq, I. Firastrau, F. Ponthenier, M. Brunet, C. Thirion, J.-P. Michel, L. Prejbeanu-Buda, M.-C. Cyrille, O. Redon, and B. Dieny, Spin-torque oscillator using perpendicular polarizer and a planar free layer, *Nat. Mater.* **6**, 447 (2007).
- [17] W. H. Rippard, A. M. Deac, M. R. Pufall, J. M. Shaw, M. W. Keller, S. E. Russek, and C. Serpico, Spin-transfer dynamics in spin valves with out-of-plane magnetized CoNi free layers, *Phys. Rev. B* **81**, 014426 (2010).
- [18] S. M. Mohseni, S. R. Sani, J. Persson, T. N. Anh Nguyen, S. Chung, Y. Pogoryelov, and J. Åkerman, High frequency operation of a spin-torque oscillator at low field, *Phys. Status Solidi RRL* **5**, 432 (2011).
- [19] S. M. Mohseni, S. R. Sani, J. Persson, T. N. Anh Nguyen, S. Chung, Ye. Pogoryelov, P. K. Muduli, E. Iacocca, A. Eklund, R. K. Dumas, S. Bonetti, A. Deac, M. Hoefler, and J. Åkerman, Spin torque-generated magnetic droplet solitons, *Science* **339**, 1295 (2013).
- [20] Y. Zhou, C. L. Zha, S. Bonetti, J. Persson, and J. Åkerman, Spin-torque oscillator with tilted fixed layer magnetization, *Appl. Phys. Lett.* **92**, 262508 (2008).
- [21] Y. Zhou, C. L. Zha, S. Bonetti, J. Persson, and J. Åkerman, Microwave generation of tilted-polarizer spin torque oscillator, *J. Appl. Phys.* **105**, 07D116 (2009).
- [22] Y. Zhou, S. Bonetti, C. L. Zha, and J. Åkerman, Zero-field precession and hysteretic threshold currents in a spin torque nano device with tilted polarizer, *New J. Phys.* **11**, 103028 (2009).
- [23] M. Albrecht, G. Hu, I. L. Guhr, T. C. Ulbrich, J. Boneberg, P. Leiderer, and G. Schatz, Magnetic multilayers on nanospheres, *Nat. Mater.* **4**, 203 (2005).
- [24] J. P. Wang, Magnetic data storage: Tilting for the top, *Nat. Mater.* **4**, 191 (2005).
- [25] U. Roy, H. Seinige, F. Ferdousi, J. Mantey, M. Tsoi, and S. K. Banerjee, Spin-transfer-torque switching in spin valve structures with perpendicular, canted, and in-plane magnetic anisotropies, *J. Appl. Phys.* **111**, 07C913 (2012).
- [26] R. Sbiaa, R. Law, E.-L. Tan, and T. Liew, Spin transfer switching enhancement in perpendicular anisotropy magnetic tunnel junction with a canted in-plane spin polarizer, *J. Appl. Phys.* **105**, 013910 (2009).

- [27] H. Zhang, W. Lin, S. Mangin, Z. Zhang, and Y. Liu, Signature of magnetization dynamics in spin-transfer-driven nanopillars with tilted easy axis, *Appl. Phys. Lett.* **102**, 012411 (2013).
- [28] Y. Zhou, H. Zhang, Y. Liu, and J. Åkerman, Macrospin and micromagnetic studies of tilted polarizer spin-torque nanoo oscillators, *J. Appl. Phys.* **112**, 063903 (2012).
- [29] Y. B. Bazaliy, Planar approximation for spin transfer systems with application to tilted polarizer devices, *Phys. Rev. B* **85**, 014431 (2012).
- [30] R. Sbiaa, Magnetization switching by spin-torque effect in off-aligned structure with perpendicular anisotropy, *J. Phys. D* **46**, 395001 (2013).
- [31] Y. F. Zheng, J. P. Wang, and V. Ng, Control of the tilted orientation of CoCrPt/Ti thin film media by collimated sputtering, *J. Appl. Phys.* **91**, 8007 (2002).
- [32] C. L. Zha, R. K. Dumas, J. Persson, S. M. Mohseni, J. Nogu, and J. Åkerman, Pseudo spin valves using a (1 1 2)-textured D022 Mn_{2.3}-2.4Ga fixed layer, *IEEE Magn. Lett.* **1**, 2500104 (2010).
- [33] C. L. Zha, J. Persson, S. Bonetti, Y. Y. Fang, and J. Åkerman, Pseudo spin valves based on L10 (111)-oriented FePt fixed layers with tilted anisotropy, *Appl. Phys. Lett.* **94**, 163108 (2009).
- [34] C. L. Zha, Y. Y. Fang, J. Nogués, and J. Åkerman, Improved magnetoresistance through spacer thickness optimization in tilted pseudo spin valves based on L10 (111)-oriented FePtCu fixed layers, *J. Appl. Phys.* **106**, 053909 (2009).
- [35] T. N. Anh Nguyen, Y. Fang, V. Fallahi, N. Benatmane, S. M. Mohseni, R. K. Dumas, and Johan Åkerman, [Co/Pd]-NiFe exchange springs with tunable magnetization tilt angle, *Appl. Phys. Lett.* **98**, 172502 (2011).
- [36] T. N. Anh Nguyen, N. Benatmane, V. Fallahi, Y. Fang, S. M. Mohseni, R. K. Dumas, and Johan Åkerman, [Co/Pd]₄-Co-Pd-NiFe spring magnets with highly tunable and uniform magnetization tilt angle, *J. Magn. Magn. Mater.* **324**, 3929 (2012).
- [37] S. Chung, S. M. Mohseni, V. Fallahi, T. N. Anh Nguyen, N. Benatmane, R. K. Dumas, and J. Åkerman, Tunable spin configuration in [Co/Ni]-NiFe spring magnets, *J. Phys. D* **46**, 125004 (2013).
- [38] F. Yildiz, M. Przybylski, and J. Kirschner, Direct evidence of a nonorthogonal magnetization configuration in single crystalline Fe_{1-x}Cox/Rh/Fe/Rh(001) system, *Phys. Rev. Lett.* **103**, 147203 (2009).
- [39] J.-M. Tonnerre, M. Przybylski, M. Ragheb, F. Yildiz, H. C. N. Tolentino, L. Ortega, and J. Kirschner, Direct in-depth determination of a complex magnetic configuration in an exchange-coupled bilayer with perpendicular and in-plane anisotropy, *Phys. Rev. B* **84**, 100407(R) (2011).
- [40] J. Choi, B.-C. Min, J.-Y. Kim, B.-G. Park, J. H. Park, Y. S. Lee, and K.-H. Shin, Non-collinear magnetization configuration in interlayer exchange coupled magnetic thin films, *Appl. Phys. Lett.* **99**, 102503 (2011).
- [41] M.-S. Lin, H.-Ch. Hou, Y.-Ch. Wu, P.-H. Huang, Ch.-H. Lai, H.-H. Lin, H.-J. Lin, and F.-H. Chang, Effect of perpendicular interlayer coupling strength on canting angles of TbCo-sublattice magnetization, *Phys. Rev. B* **79**, 140412 (R) (2009).
- [42] H.-C. Hou, B. J. Kirby, K. Z. Gao, and C.-H. Lai, Characterizing formation of interface domain wall and exchange coupling strength in laminated exchange coupled composites, *Appl. Phys. Lett.* **102**, 162408 (2013).
- [43] R. K. Dumas, Y. Fang, B. J. Kirby, C. L. Zha, V. Bonanni, J. Nogués, and Johan Åkerman, Probing vertically graded anisotropy in FePtCu films, *Phys. Rev. B* **84**, 054434 (2011).
- [44] R. Law, R. Sbiaa, T. Liew, and T. C. Chong, Effect of Ta seed layer and annealing on magnetoresistance in CoFe/Pd-based pseudo-spin-valves with perpendicular anisotropy, *Appl. Phys. Lett.* **91**, 242504 (2007).
- [45] T. Tahmasebi, S. N. Piramanayagam, R. Sbiaa, R. Law, and T. C. Chong, Effect of different seed layers on magnetic and transport properties of perpendicular anisotropic spin valves, *IEEE Trans. Magn.* **46**, 1933 (2010).
- [46] O. Hellwig, T. Hauet, T. Thomson, E. Dobisz, J. D. Risner-Jamgaard, D. Yaney, B. D. Terris, and E. E. Fullerton, Coercivity tuning in Co/Pd multilayer based bit patterned media, *Appl. Phys. Lett.* **95**, 232505 (2009).
- [47] T. Hauet, E. Dobisz, S. Florez, J. Park, B. Lengsfeld, B. D. Terris, and O. Hellwig, Role of reversal incoherency in reducing switching field and switching field distribution of exchange coupled composite bit patterned media, *Appl. Phys. Lett.* **95**, 262504 (2009).
- [48] R. Nakajima, J. Stöhr, and Y. U. Idzerda, Electron-yield saturation effects in L-edge x-ray magnetic circular dichroism spectra of Fe, Co, and Ni, *Phys. Rev. B* **59**, 6421 (1999).
- [49] J. Stöhr, X-ray magnetic circular dichroism spectroscopy of transition metal thin films, *J. Electron Spectrosc. Relat. Phenom.* **75**, 253 (1995).
- [50] J. Stöhr, Exploring the microscopic origin of magnetic anisotropies with x-ray magnetic circular dichroism (XMCD) spectroscopy, *J. Magn. Magn. Mater.* **200**, 470 (1999).
- [51] B. T. Thole, P. Carra, F. Sette, and G. van der Laan, X-ray circular dichroism as a probe of orbital magnetization, *Phys. Rev. Lett.* **68**, 1943 (1992).
- [52] P. Carra, B. T. Thole, M. Altarelli, and X. Wang, X-ray circular dichroism and local magnetic fields, *Phys. Rev. Lett.* **70**, 694 (1993).
- [53] R. Wu and A. J. Freeman, Limitation of the magnetic-circular-dichroism spin sum rule for transition metals and importance of the magnetic dipole term, *Phys. Rev. Lett.* **73**, 1994 (1994).
- [54] H. A. Dürr, G. van der Laan, and B. T. Thole, Comment on "Microscopic origin of magnetic anisotropy in Au/Co/Au probed with x-ray magnetic circular dichroism", *Phys. Rev. Lett.* **76**, 3464 (1996).
- [55] D. Weller, J. Stöhr, R. Nakajima, A. Carl, M. G. Samant, C. Chappert, R. Mégy, P. Beauvillain, P. Veillet, and G. A. Held, Microscopic origin of magnetic anisotropy in Au/Co/Au probed with x-ray magnetic circular dichroism, *Phys. Rev. Lett.* **75**, 3752 (1995).
- [56] J. Stöhr and H. König, Determination of spin-density and orbital-moment anisotropies in transition metals with angle dependent x-ray magnetic circular dichroism, *Phys. Rev. Lett.* **75**, 3748 (1995).
- [57] F. Wilhelm, P. Pouloupoulos, P. Srivastava, H. Wende, M. Farle, K. Baberschke, M. Angelakeris, N. K. Flevaris,

- W. Grange, J.-P. Kappler, G. Ghiringhelli, and N.B. Brookes, Magnetic anisotropy energy and the anisotropy of the orbital moment of Ni in Ni/Pt multilayers, *Phys. Rev. B* **61**, 8647 (2000).
- [58] T. Leineweber and H. Kronmüller, Micromagnetic examination of exchange coupled ferromagnetic nanolayers, *J. Magn. Magn. Mater.* **176**, 145 (1997).
- [59] D.-T. Ngo, Z. L. Meng, T. Tahmasebi, X. Yu, E. Thoeng, L. H. Yeo, G. C. Han, and K.-L. Teo, Interfacial tuning of perpendicular magnetic anisotropy and spin magnetic moment in CoFe/Pd multilayers, *J. Magn. Magn. Mater.* **350**, 42 (2014).
- [60] S.-C. Shin, G. Srinivas, Y.-S. Kim, and M.-G. Kim, Observation of perpendicular magnetic anisotropy in Ni/Pt multilayers at room temperature, *Appl. Phys. Lett.* **73**, 393 (1998).
- [61] S. Y. Jang, C.-Y. You, S. H. Lim, and S. R. Lee, Annealing on the magnetic dead layer and saturation magnetization in unit structures relevant to a synthetic ferrimagnetic free structure, *J. Appl. Phys.* **109**, 013901 (2011).